NONCONFORMING MIXED FINITE ELEMENT METHODS ON POLYHEDRAL MESHES

Yuri Kuznetsov

Department of Mathematics
University of Houston

Moscow
June, 2017

Outline

- problem formulation
- nonmatching meshes
- mortar element method
- KR-method
- another polyhedral FE method
- FE method with piecewise constant fluxes (2007-2011)
- meshes with mixed macro-cells
- new interface condition
- nonconforming meshes

Problem formulation

Let Ω be a polygonal (in R^2) or polyhedral (in R^3) domain. In Ω we consider the diffusion problem in the mixed formulation:

$$\begin{aligned} D^{-1}\mathbf{u} \; + \; \mathrm{grad}\; p \; &= \; 0 \text{ in } \Omega \\ -\,\mathrm{div}\; \mathbf{u} \; - \; cp \; &= \; -f \text{ in } \Omega \\ \mathbf{u}\cdot\mathbf{n} \; &= \; 0 \text{ on } \partial\Omega \end{aligned} \tag{1}$$

Problem formulation

The equivalent weak (variational) formulation of (1) is as follows:
Find $\mathbf{u} \in H_{\mathrm{div}}(\Omega),\ \mathbf{u}\cdot\mathbf{n} = 0$ on $\partial\Omega,\ p \in L_2(\Omega)$, such that

$$
\begin{array}{rcrcr}
\int_\Omega (D^{-1}\mathbf{u})\cdot\mathbf{v}\,\mathrm{d}x & + & \int_\Omega (\nabla\mathbf{v})\cdot p\,\mathrm{d}x & = & 0, \\
-\int_\Omega (\nabla\mathbf{u})\cdot q\,\mathrm{d}x & - & \int_\Omega c\cdot p\cdot q\,\mathrm{d}x & = & -\int_\Omega f\cdot q\,\mathrm{d}x
\end{array}
$$

for all $\mathbf{v} \in H_{\mathrm{div}}(\Omega),\ \mathbf{v}\cdot\mathbf{n} = 0$ on $\partial\Omega,\ q \in L_2(\Omega)$
Here $D = D(\mathbf{x})$ is a symmetric positive definite matrix and $c = c(x)$ is a nonnegative function for any $\mathbf{x} \in \Omega$.

Differential Macro-Hybrid Problem

Let Ω be covered by polygonal/polyhedral conforming mesh Ω_H with macro-cells $E_1, E_2, \ldots, E_N,\ N > 1$. The corresponding differential macro-hybrid mixed formulation is as follows: Find the vector-functions $\mathbf{u}_s$, functions p_s and $\lambda_{s,t}$, $s < t,\ s, t \in \overline{1, N}$, such that

$$
\begin{array}{ccccccc}
D_s^{-1}\mathbf{u}_s & + & \mathrm{grad}\ p_s & = & 0 & & \text{in } E_s, \\
-\mathrm{div}\ \mathbf{u}_s & - & c\ p_s & = & -f & & \text{in } E_s, \\
\lambda_{s,t} & \equiv & p_s & \equiv & p_t & & \text{a.e on } \Gamma_{s,t}\,, \\
\mathbf{u}_s \cdot \mathbf{n}_s & + & \mathbf{u}_t \cdot \mathbf{n}_t & = & 0 & & \text{a.e on } \Gamma_{s,t}\,, \\
 & & \mathbf{u}_s \cdot \mathbf{n}_s & = & 0 & & \text{a.e on } \partial E_s \cap \partial\Omega\,,
\end{array}
$$

$$
s < t,\ \ s, t = \overline{1, N},
$$

where ∂E_s is the boundary of E_s, $\Gamma_{s,t} = \partial E_s \cap \partial E_t$ and $\mathbf{n}_s$ is the outward unit normal to $\partial E_s,\ \ s = \overline{1, N}$.

Prismatic Cluster as a Macro-Cell

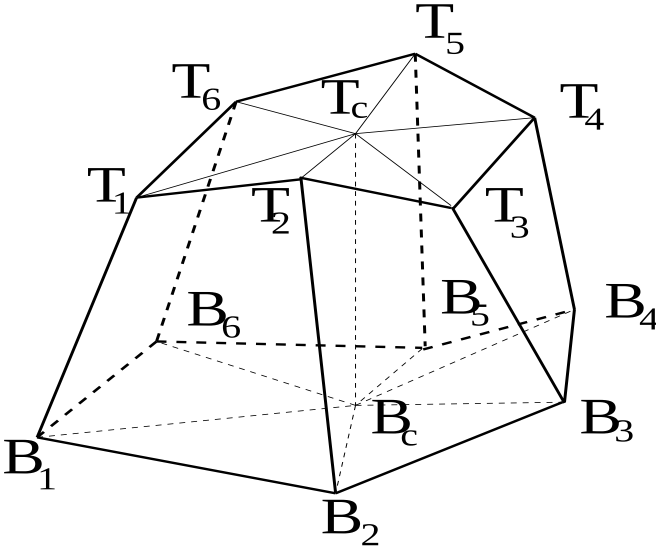

Polyhedral Mesh Cells

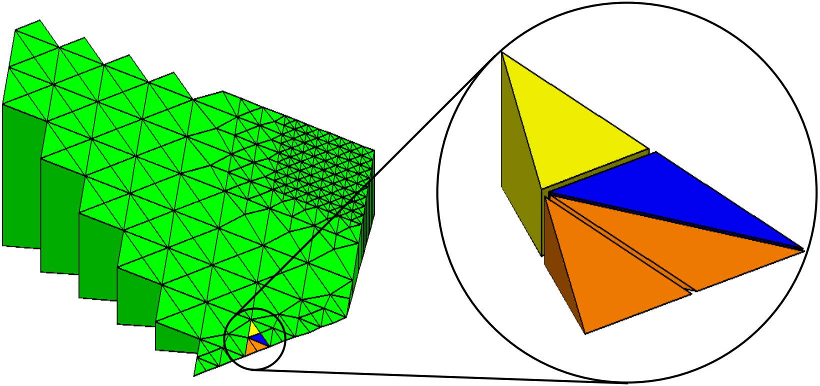

Degenerated Macro-Cell

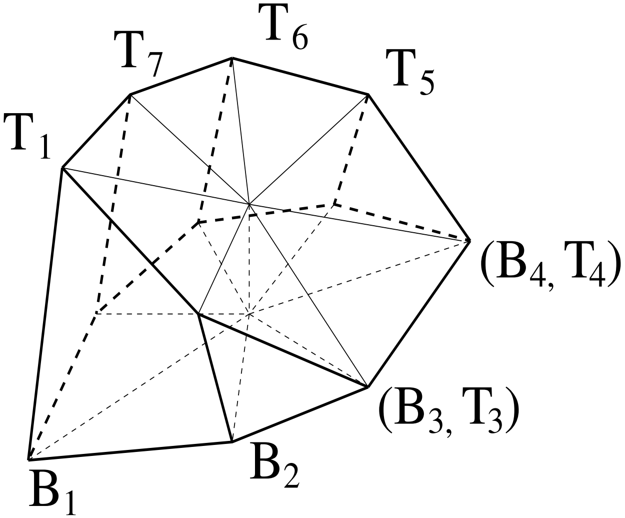

Non-Matching Meshes on Faults

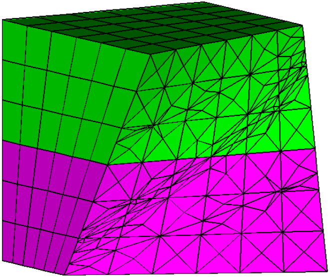

Left subdomain

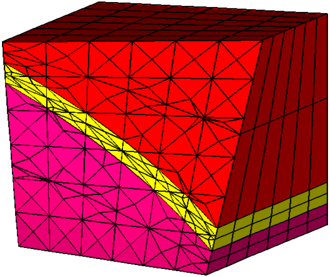

Right subdomain

Example of a Distorted Hexahedral Mesh Cell on a Fault Surface: Non-matching, or Nonconforming Polyhedral Meshes

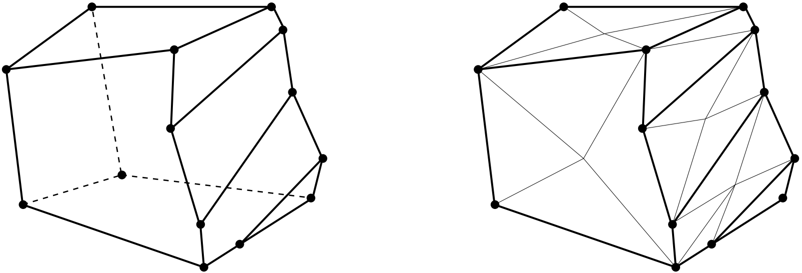

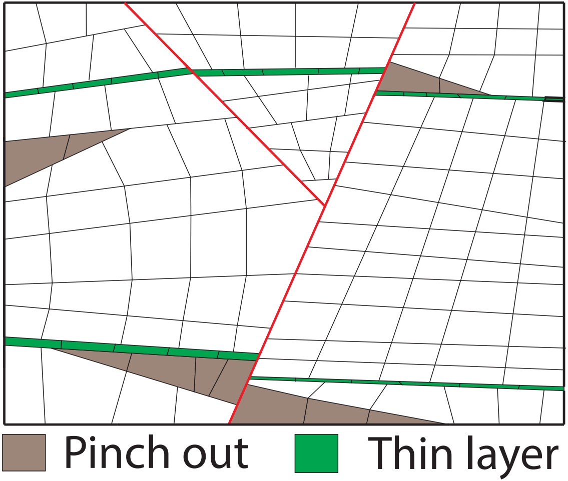
Pinch out
Thin layer

The equivalent variational mixed macro-hybrid formulation is:
Find $\mathbf{u}_s \in V_s,\ p_s \in Q_s,\ \lambda_{st} \in \Lambda_{st}$ such that

$$\int_{E_s} (D^{-1}\mathbf{u}_s) \cdot \mathbf{v}_s \, \mathrm{d}x - \int_{E_s} p_s \cdot (\nabla \cdot \mathbf{v}_s) \, \mathrm{d}x$$

$$- \sum_{t=1}^{s-1} \int_{\Gamma_{ts}} (\mathbf{v}_s \cdot \mathbf{n}_s)\lambda_{ts} \, \mathrm{d}l \ + \ \sum_{t=s+1}^{N} \int_{\Gamma_{st}} (\mathbf{v}_s \cdot \mathbf{n}_s)\lambda_{ts} \, \mathrm{d}l \ = 0,$$

$$- \int_{E_s} (\nabla \mathbf{u}_s) \cdot q_s \, \mathrm{d}x - \int_{E_s} c \cdot p_s \cdot q_s \, \mathrm{d}x = - \int_{E_s} f \cdot q_s \, \mathrm{d}x$$

$$\forall \ (\mathbf{v}_s, q_s) \in V_s \times Q_s, \ \ s = \overline{1, N},$$

Matching interface conditions

$$\int_{\Gamma_{st}} \mu_{st}(\mathbf{u}_s \cdot \mathbf{n}_s \; + \mathbf{u}_t \cdot \mathbf{n}_t)\,\mathrm{d}l = 0$$

$$\forall \mu_{st} \in \Lambda_{s,t},\;\; s < t,\;\; s,t = \overline{1,N}.$$

Here,

$$V_s = \{\mathbf{v} : \mathbf{v} \in H_{\mathrm{div}}(\Omega_s), \mathbf{v} \cdot \mathbf{n}_s = 0 \text{ on } \partial\Omega\},$$

$$Q_s = L_2(\Omega_s),\;\; \Lambda_{s,t} = L_2(\Gamma_{s,t}),$$

$$s < t,\;\; s,t = \overline{1,N}.$$

Saddle-point quadratic functional

Let us define the variational functional

$$J(\overline{\mathbf{v}}, \overline{q}) = \sum_{s=1}^{N} J_s(\mathbf{v}_s, q_s),$$

where

$$J_s(\mathbf{v}_s, q_s) = \frac{1}{2}\int_{E_s} (D^{-1}\mathbf{v}_s) \cdot \mathbf{v}_s \, \mathrm{d}x \; - \; \int_{E_s} q_s \cdot (\nabla \cdot \mathbf{v}_s) \, \mathrm{d}x \; - \\ \frac{1}{2}\int_{E_s} c \cdot q_s^2 \, \mathrm{d}x - \int_{E_s} f q_s \, \mathrm{d}x,$$

$\mathbf{v}_s \in V_s, \; q_s \in Q_s, \; s = \overline{1, N}$.

Another variational problem

It is well known that the above variational problem is equivalent to another variational problem: Find $\mathbf{u} \in V$, $\overline{p} \in Q$, such that:

$$J(\overline{\mathbf{u}}, \overline{p}) = \inf_{\overline{\mathbf{v}} \in V} \sup_{\overline{p} \in Q} J(\overline{\mathbf{v}}, \overline{p}),$$

where

$$V = \Big\{ \overline{\mathbf{v}} = (\mathbf{v}_1, \ldots, \mathbf{v}_N) : \mathbf{v}_s \in V_s, \; s = \overline{1, N},$$

$$\int_{\Gamma_{st}} \mu_{st} (\mathbf{u}_s \cdot \mathbf{n}_s \; + \mathbf{u}_t \cdot \mathbf{n}_t) \, \mathrm{d}l = 0, \; \forall \mu_{st} \in \Lambda_{s,t}, \; s < t, \; s, t = \overline{1, N} \Big\},$$

$$Q = \Big\{ \overline{q} = (q_1, \ldots, q_N) : q_s \in Q_s, \; s = \overline{1, N} \Big\}.$$

Nonmatching meshes by mortar element method

International collaboration in 1992-2000

- France: Y. Achdou, O. Pironneau (University Paris-6), J. Periaux (Dassault Aviation)
  A. Bespalov, K. Lipnikov, Yu. K.
- Germany: R. Hoppe, B, Wohlmuth (Ausburg University)
  Yu. Vassilevski, Yu. Iliash, Yu. K.
- USA: M. Wheeler, I. Yotov (Rise University/UT Austin)
  Yu. Vassilevski, Yu. K.

The original Idea(2003)

1. To partition each macro-cell E_s into simple shape subcells $\{e_{s,i}\}$.
2. To use a discretization methods in subcells.
3. To impose matching conditions on the interfaces between macro-cells.
4. To eliminate DOFs for normal fluxes in subcells.
5. To sub-assemble the submatrices inside macro-cells and for the whole macro-mesh.

Restrictions in Industrial applications:

– in each macro-cell should be only one "cell-centred" DOF for the solution function;

– on each interface should be only one DOF for the normal flux.

Let $E_{s,h}$ be a conformal triangular/tetrahedral mesh in E_s and $\widetilde{\mathbf{V}}_{s,h} \subset H_{\mathrm{div}}(E_s)$ be the lowest order Raviart-Thomas (RT_0) FE space. Let

$$\mathbf{V}_{s,h} = \{\mathbf{v} \in \widetilde{\mathbf{V}}_{s,h},$$

$$\mathbf{v} \cdot \mathbf{n}_s = 0 \text{ a.e. on } \partial E_s \cap \partial\Omega,$$

$$\nabla \cdot \mathbf{v} \equiv \text{const a.e. in } E_s,$$

$$\mathbf{v}_{h,s} \cdot \mathbf{n}_s \equiv \text{const}_{st} \text{ a.e. on } \Gamma_{s,t} = \partial E_s \cap \partial E_t,\ \ s \neq t\},$$

$$s = \overline{1, N},$$

Kuznetsov, Repin (KR, 2003)

$$\mathbf{V}_h = \Big\{\bar{\mathbf{v}} = (\mathbf{v}_1, \mathbf{v}_2, \ldots, \mathbf{v}_N) : \mathbf{v}_s \in \mathbf{V}_{s,h}\ s = \overline{1, N},$$
$$\mathbf{v}_s \cdot \mathbf{n}_s + \mathbf{v}_t \cdot n_t = 0 \text{ a.e. on } \Gamma_{s,t},\ \ s \neq t\big\}\,,$$

$$Q_h = \{\bar{q} = (q_1, q_2, \ldots, q_N) : q_s \equiv \text{const in } E_s\ \ s = \overline{1, N}\}.$$

Kuznetsov, Repin (KR, 2003)

KR - method: Find $\overline{\mathbf{u}}_h \in V_h,\ \overline{p} \in Q_h$ such that

$$J\left(\overline{\mathbf{u}}_h, \overline{p}\right) = \inf_{\overline{\mathbf{v}} \in V_h} \sup_{\overline{q} \in Q_h} J\left(\overline{\mathbf{v}}, \overline{q}\right)$$

Remark: KR was intensively used in experimental codes at URC ExxonMobil and at INRIA by J.Jaffre $\&$ Team.

Algebraic system

$$\begin{pmatrix} M & B^T & C^T \\ B & -\Sigma & 0 \\ C & 0 & 0 \end{pmatrix} \begin{pmatrix} \overline{u} \\ \overline{p} \\ \overline{\lambda} \end{pmatrix} = \begin{pmatrix} 0 \\ -\overline{F} \\ 0 \end{pmatrix}$$

Condensed system by eliminating $\overline{u}$:

$$\widehat{S}_{p\lambda} \begin{pmatrix} \overline{p} \\ \overline{\lambda} \end{pmatrix} \equiv \begin{pmatrix} S_{pp} & S_{p\lambda} \\ S_{\lambda p} & S_{\lambda\lambda} \end{pmatrix} \begin{pmatrix} \overline{p} \\ \overline{\lambda} \end{pmatrix} = \begin{pmatrix} -\overline{F} \\ 0 \end{pmatrix}, \quad \widehat{S}_{p\lambda} = \widehat{S}_{p\lambda}^T \geqslant 0$$

Remark: Matrix M is block-diagonal: one block per a macro cell.

Example of a Mixed macro-cell

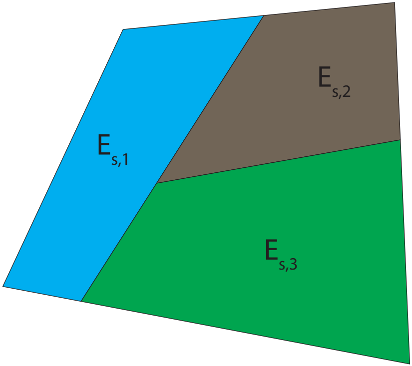

Mixed macro-cells arise in interdisciplinary problems, for instance, high temperature gas dynamics coupled with heat diffusion. Partitioning of E_s into $E_{s,i},\ i = 1, \ldots,$ is based on information from previous time-steps and the "volume fraction" condition (LANL).

Drawback of the KR-method

In mixed macro-cells the condition

$$\text{div } \mathbf{u}_s \equiv \text{const}$$

does not work in case of strongly contrast materials.

Let $E_{s,h} = \{e_{s,i}\}_{i=1}^{n_s}$ be a triangular/tetrahedral mesh in E_s, $s = \overline{1, N}$. Then we define

$$\mathbf{V}_{s,h} = \{\mathbf{v} \in \widetilde{\mathbf{V}}_{s,h},\ \mathbf{v} \cdot \mathbf{n}_s = 0,\ \text{a.e. on } \partial E_s \cap \partial\Omega,$$
$$\mathbf{v}_{s,h} \cdot \mathbf{n}_s \equiv \text{const}_{st} \text{ a.e. on } \Gamma_{s,t},\ s \neq t\},\ s = \overline{1, N},$$

$$\mathbf{V}_h = \{\bar{\mathbf{v}} = (\mathbf{v}_1, \mathbf{v}_2, \ldots, \mathbf{v}_N) : \mathbf{v}_s \in \mathbf{V}_{s,h}\ s = \overline{1, N},$$
$$\mathbf{v}_s \cdot \mathbf{n}_s + \mathbf{v}_t \cdot \mathbf{n}_t = 0 \text{ a.e. on } \Gamma_{s,t},\ s \neq t\},$$

$$Q_{s,h} = \{q_s : q_s \equiv \text{const in each } e \in E_{s,h}\},$$

$$Q_h = \{\bar{q} = (q_1, q_2, \ldots, q_N) : q_s \in Q_{s,h}\ s = \overline{1, N}\}.$$

Another macro-hybrid method (Kuznetsov, 2005)

After eliminating of the "interior" DOFs for $u_{s,h} \in V_{s,h}$ and DOFs for $p_{s,h} \in Q_{s,h}$ the algebraic saddle point problem can be transformed into system

$$\begin{pmatrix} \widetilde{M} & B^T & C^T \\ B & -\Sigma & 0 \\ C & 0 & 0 \end{pmatrix} \begin{pmatrix} \overline{u}_H \\ \overline{p}_H \\ \overline{\lambda}_H \end{pmatrix} = \begin{pmatrix} 0 \\ -\overline{G} \\ 0 \end{pmatrix}$$

with the KR matrices B, C and Σ and with different matrices $\widetilde{M} \neq M$ and with the new right hand side vector $\overline{G} \neq \overline{F}$. Here $\overline{p}_H^T = (p_q, \ldots, p_N)$,

$$p_s = \frac{1}{|E_s|} \sum_{i=1}^{n_s} p_{s,i} |e_{s,i}|$$

and $\overline{u}_H \in \mathbb{R}^m$, where m is the total number of interfaces between macro-cells.

<u>Remark</u>: The method was intensively used in the production code at Los Alamos NL.

PWCF discretization vs RT_0 method (Kuznetsov, 2007)

Drawbacks of RT_0 discretization inside polyhedral macro-cells:

- The matrix M in RT_0 discretization may be very ill-conditioned: anisotropic tetrahedrons, anisotropic diffusion tensor, and combination of both. In practical situations we observed Cond $M > 10^{15}$, $s \geqslant 1$.
- In the case of many tetrahedrons in E_s calculation of M_s could be rather expensive.

  In practical codes we replace RT_0 discretization by newly developed FE method with piece-wise constant fluxes (PWCF-method).

Discontinuous Galerkin on quadrilateral meshes (Kuznetsov, 2007)

Let E_k and E_l be quadrilaterals with the common interface $\Gamma = \Gamma_{kl}$:

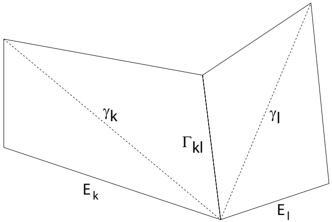

or

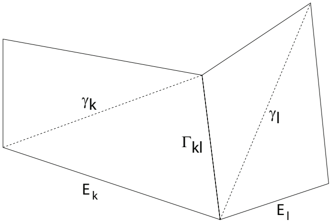

We partition E_k and E_l into triangles with faces γ_k and γ_l, respectively, as shown above.

Discontinuous Galerkin on quadrilateral meshes (Kuznetsov, 2007)

Let $\omega \equiv \omega_\Gamma$ be the union of two triangles with the common interface Γ_{kl}:

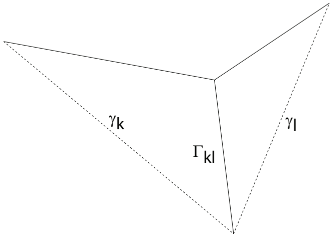

or

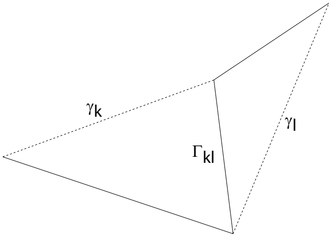

Let $\mathbf{n}_\Gamma$ be the unit normal to Γ_{kl} directed from E_k into E_l, and $\mathbf{w}$ be the piecewise constant vector field defined as follows:

1. $\mathbf{w}$ is constant in $E_k \cap \omega$ and $E_l \cap \omega$
2. $\mathbf{w} \cdot \mathbf{n}_\Gamma = 1$ on Γ
3. $\mathbf{w} \cdot \mathbf{n} = 0$ on $\partial\omega \cap \partial E_k \setminus \Gamma$ and $\partial\omega \cap \partial E_l \setminus \Gamma$

Discontinuous Galerkin on quadrilateral meshes (Kuznetsov, 2007)

Let $\mathbf{u}^*$, p^* be the exact solution of the original problem:

$$D^{-1}\mathbf{u}^* + \nabla p^* = 0 \quad \text{in } \omega\,.$$

Consider the exact algebraic equation

$$\int_\omega \left(D^{-1}\mathbf{u}^*\right)\mathbf{w}\,\mathrm{d}x + \int_\omega (\nabla p^*)\cdot\mathbf{w}\,\mathrm{d}x \equiv$$
$$\equiv \int_\omega \left(D^{-1}\mathbf{u}^*\right)\mathbf{w}\,\mathrm{d}x + \int_{\partial\omega} (\mathbf{n}_\omega\cdot\mathbf{w})\,p^*\,\mathrm{d}s = 0\,.$$

Discontinuous Galerkin on quadrilateral meshes (Kuznetsov, 2007)

It can be easily shown that

$$\int_{\partial\omega} (\mathbf{n}_\omega \cdot \mathbf{w})\, p^*\, \mathrm{d}s \;=\; |\Gamma|\, (p_k^* - p_l^*)\,,$$

where

$$p_k^* \;=\; \frac{1}{|\gamma_k|} \int_{\gamma_k} p^*\, \mathrm{d}s\,, \quad p_l^* \;=\; \frac{1}{|\gamma_l|} \int_{\gamma_l} p^*\, \mathrm{d}s\,.$$

Thus, we get the exact equation

$$\int_\omega \left(D^{-1}\mathbf{u}^*\right) \mathbf{w}\, \mathrm{d}x \;+\; |\Gamma|\, (p_k^* - p_l^*) \;=\; 0\,.$$

Remark: The latter formula looks like the two-point discretization of the normal flux at Γ.

Discontinuous Galerkin on quadrilateral meshes (Kuznetsov, 2007)

Now, we define the bilinear forms

$$a(\mathbf{u},\, \mathbf{v}) \;=\; \int_\Omega \left(D^{-1}\mathbf{u}\right)\mathbf{v}\,\mathrm{d}x \quad \text{and} \quad b(p,\, \mathbf{v}) \;=\; \sum_{k<l} |\Gamma_{kl}|\left(p_k - p_l\right) v_{kl},$$

where

$$p_k \;=\; \frac{1}{|\gamma_k|}\int_{\gamma_k} p\,\mathrm{d}s\,, \quad v_{kl} \;=\; \frac{1}{|\Gamma_{kl}|}\int\limits_{\Gamma_{kl}} \mathbf{v}\cdot\mathbf{n}_{kl}\,\mathrm{d}s\,.$$

Discontinuous Galerkin on quadrilateral meshes (Kuznetsov, 2007)

We have proved that $\mathbf{u}^*$, p^* satisfy the equations

$$\begin{array}{rcccl} a(\mathbf{u}^*,\ \mathbf{v}) & + & b(p^*_{h,\mathsf{int}},\ \mathbf{v}) & = & 0\,, \\ b(q,\ \mathbf{u}^*_{h,\mathsf{int}}) & & & = & l(q)\,, \end{array}$$

where

$$l(q) \;=\; -\int_\Omega f\,q\,\mathsf{d}x$$

for any $\mathbf{v} \in W_h$ and $q \in Q_h$.

Discontinuous Galerkin on quadrilateral meshes (Kuznetsov, 2007)

Then, the Discontinuous Galerkin method with PWC fluxes reads of follows:

Find $\mathbf{u}_h \in W_h$, $p_h \in Q_h$ such that

$$\begin{array}{rcl} a(\mathbf{u}_h,\ \mathbf{v}) \;+\; b(p,\ \mathbf{v}) & = & 0, \\ b(q,\ \mathbf{u}_h) & = & l(q) \end{array}$$

for any $\mathbf{v} \in W_h$, $q \in Q_h$.

Error estimate for PWC fluxes (Kuznetsov, 2011)

Using the previously described operations, we can easily prove that

$$a\left(\mathbf{u}^* - \mathbf{u}_h,\ \mathbf{u}^*_{h,\mathsf{int}} - \mathbf{u}_h\right) \;=\; 0\,,$$

which is equivalent to

$$\|\mathbf{u}^*_h - \mathbf{u}_h\|^2_{D^{-1}} \;=\; a\left(\mathbf{u}^*_h - \mathbf{u}^*,\ \mathbf{u}^*_h - \mathbf{u}_h\right)$$

and results in the estimate

$$\|\mathbf{u}^* - \mathbf{u}_h\|_{D^{-1}} \leq 2\|\mathbf{u}^* - \mathbf{u}^*_{h,\mathsf{int}}\|_{D^{-1}}\,.$$

Remark: The latter estimation was extended to the above two macro-hybrid methods with both RT_0 and PWCF methods inside macro-cells.

Error estimate for PWC fluxes (Kuznetsov, 2011)

Mesh cells in 2D

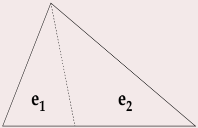

triangle

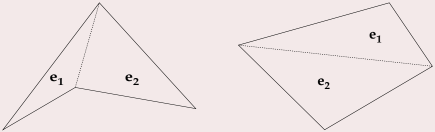

quadrilaterals

Mesh cells in 3D

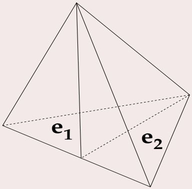

tetrahedron

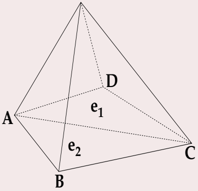

pyramid with a flat polygon ABCD

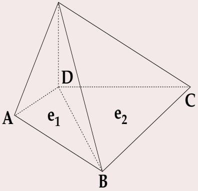

pyramid with a broken polygon ABCD

Drawback of the above methods

The methods with constant normal fluxes on the interfaces between macro-cells don't work in two important cases:

- strongly "broken" interfaces;
- mixed macro-cells with several contrast materials on interfaces.

Numerical Example

Parameters

Domain: $\Omega = (-1, 1) \times (0, 2)$
Mesh: Ω_h 25×25 cells $h_x = h_y = 0.8$
Time Step: $\delta t = 0.005$

Subdomains: interleaving strips with $k_1 = 10^{-12}$ and $k_2 = 1$
Problem:

$$-\nabla \left(K \nabla T^k \right) + \frac{T^k}{\triangle t} = \frac{T^{k-1}}{\triangle t},$$

$$\begin{aligned} T &= 1 \text{ on } \partial\Omega \cap (y = 0), \\ T &= 0 \text{ on } \partial\Omega \cap (y = 2), \\ (K \nabla T) \cdot \mathbf{n} &= 1 \text{ on } \partial\Omega \cap (x = -1),\ \partial\Omega \cap (x = 1), \\ T^0 &= 0 \text{ on } \Omega. \end{aligned}$$

Square mesh with mixed macro-cells

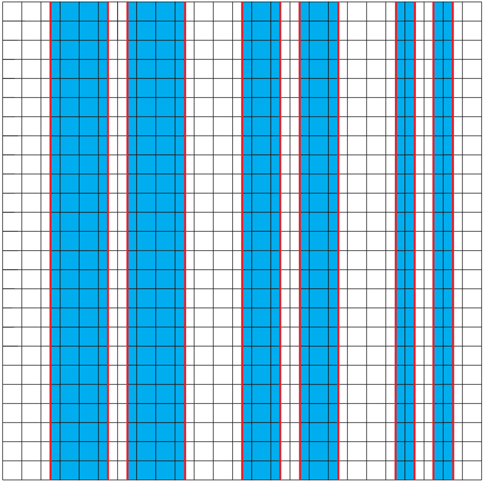

Old conforming approximation

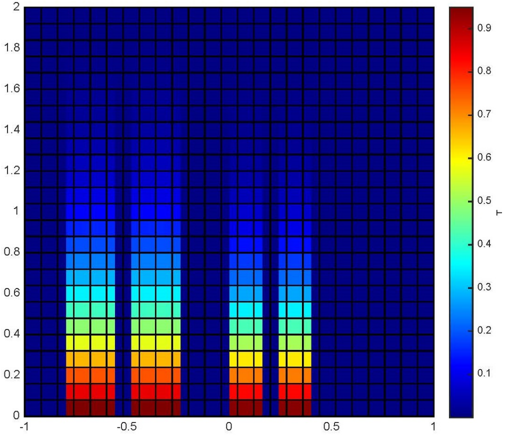

New nonconforming method

$V_{s,h}$ for E_s are the same, $s = \overline{1, N}$. The new FE space is based on the continuity of the total fluxes on the interfaces between macro-cells:

$$\mathbf{V}_h = \Big\{ \bar{\mathbf{v}} = (\mathbf{v}_1, \mathbf{v}_2, \ldots, \mathbf{v}_N) : \mathbf{v}_s \in \mathbf{V}_{s,h},\ s = \overline{1, N},$$
$$\int_{\Gamma_{s,t}} \mathbf{v}_s \cdot \mathbf{n}_s + \int_{\Gamma_{s,t}} \mathbf{v}_t \cdot n_t = 0 \text{ a.e. on } \Gamma_{s,t},\ s \neq t \Big\},$$

Q_h is the same.

New nonconforming approximation

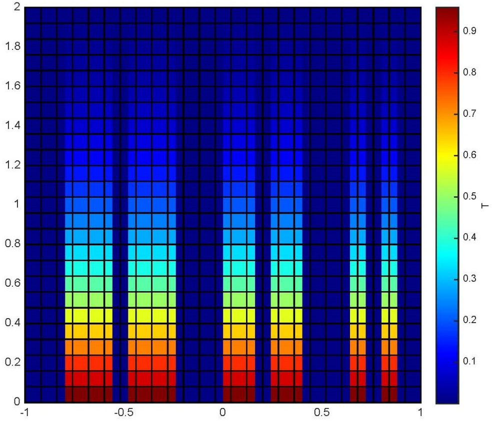

Accuracy of solutions

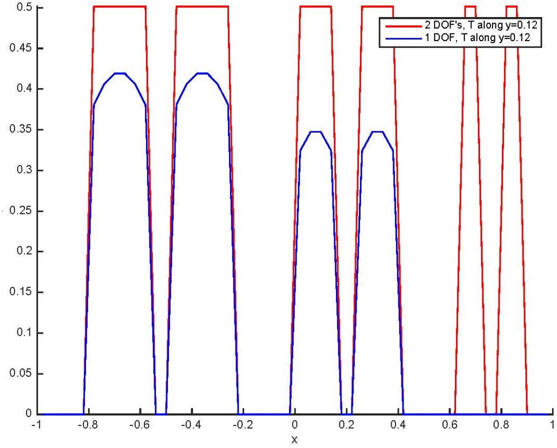

Non-conforming meshes

In theoretical research, a mesh is said to be conforming if any two adjacent mesh cells satisfy the condition:

- "vertex-to-vertex";
- "edge-to-edge";
- "face-to-face".

Otherwise, the meshes are said to be non-conforming. For instance, non-matching meshes,generally speaking, are non-conforming ones. In practice, very often we have to use non-conforming meshes $\Omega_H = \bigcup_{s=1}^{m} \overline{E}_s$ such that either $|E_s \cap E_t| \neq 0$ for some $s \neq t$ or $\Omega_H \neq \overline{\Omega}$, or both.

An Example of the Original Conforming Mesh

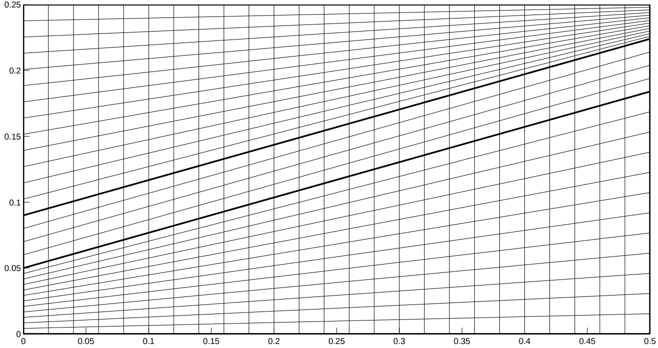

Figure: An example of the initial conforming mesh

An example of a non-conforming mesh

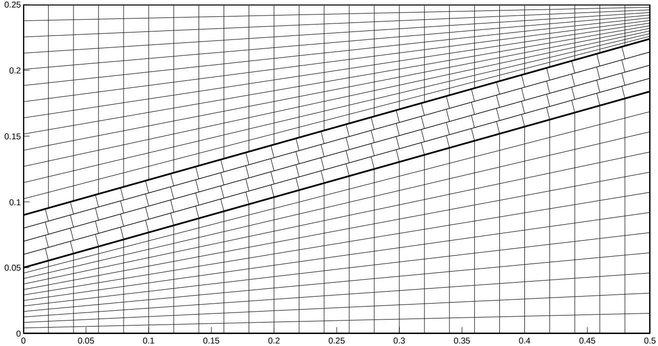

Figure: An example of a non-conforming mesh

"Logically" Conforming Meshes

An example:

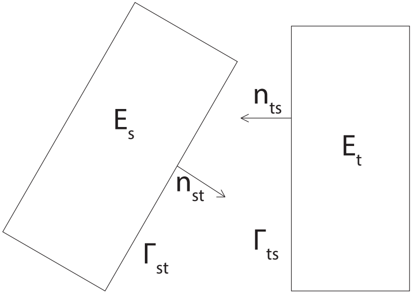

Flux matching conditions:

$$\int_{\Gamma_{st}} (\nabla \mathbf{u}_s) \cdot \mathbf{n}_{st}\, \mathrm{d}l + \int_{\Gamma_{ts}} (\nabla \mathbf{u}_t) \cdot \mathbf{n}_{ts}\, \mathrm{d}l \;=\; 0.$$

Relative Errors

Table: Relative error in PWC discrete solution $\boldsymbol{w}_h^{PWC}$, %, for angle $\alpha = 45^\circ$, conforming mesh

	G_1	G_2	G_3
$4\boldsymbol{h}$	6.47516	5.9941	5.98602
$2\boldsymbol{h}$	3.23569	2.02823	2.98601
$\boldsymbol{h}$	1.61761	0.842736	1.49213

Table: Relative error in PWC discrete solution $\boldsymbol{w}_h^{PWC}$, %, for angle $\alpha = 45^\circ$, non-conforming mesh

	G_1	G_2	G_3
$4\boldsymbol{h}$	6.47512	5.9229	5.98567
$2\boldsymbol{h}$	3.23567	1.96789	2.98584
$\boldsymbol{h}$	1.6176	0.812716	1.49205

Domain G and Mesh G_h for Mesh Step Size $4\boldsymbol{h}$, $(x_C,\ y_C) = (-1.475,\ 0.05)$

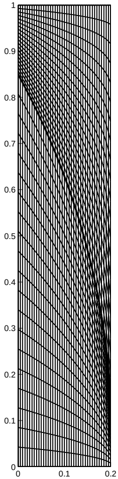

Figure: Domain G and mesh G_h for mesh step size $4\boldsymbol{h}$, $(x_C,\ y_C) = (-1.475,\ 0.05)$

Mesh Cell Inside $G_{h,2}$ for Angle $\alpha = 85^\circ$ and Mesh Step Size $2h$, Non-Conforming Mesh

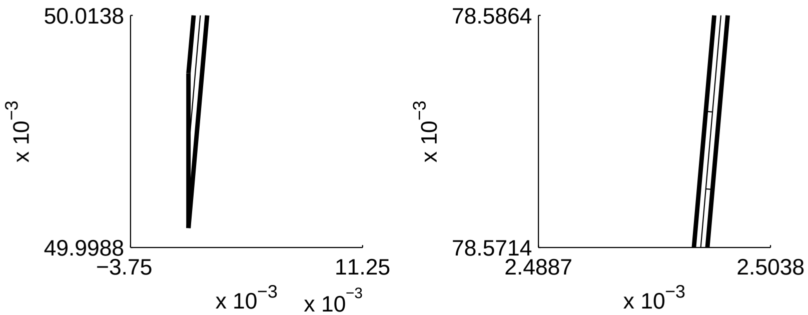

Figure: Mesh cell inside $G_{h,2}$ for angle $\alpha = 85^\circ$ and mesh step size $2h$, non-conforming mesh

Table: Relative error in PWC discrete solution w_h^{PWC}, in %, for angle $\alpha = 85^\circ$, conforming mesh

	G_1	G_2	G_3
$4h$	5.11235	9.58808	4.74141
$2h$	2.54404	2.98806	2.35079
h	1.27059	1.06517	1.17285

Table: Relative error in PWC discrete solution w_h^{PWC}, in %, for angle $\alpha = 85^\circ$, non-conforming mesh

	G_1	G_2	G_3
$4h$	5.11111	8.61626	4.73696
$2h$	2.54334	2.02273	2.34864
h	1.27043	0.905955	1.1724

Acknowledgements

This research was supported by:

- Exxon Mobil Upstream Research Company;
- The Department of Energy / Los Alamos.

The author is grateful to E.Kikinzon and V.Kramarenko for their assistance in the preparation of this talk.